The theory of transverse-unhomogeneous beam-plasma amplifiers

M. V. Kuzelev, V. A. Panin, A. P. Plotnikov, and A. A. Rukhadze

M. V. Lomonosov State University, Moscow

(Submitted 2 July 1991)
Zh. Eksp. Teor. Fiz. **101**, 460–478 (February 1992)

In this paper we present a theoretical treatment of linear and nonlinear amplification of electromagnetic waves in a magnetized beam-plasma system of general form with transverse density variation. Analytical and numerical methods are used to calculate the field amplitude, conversion efficiency of beam energy into energy of radiation, and radiated power, as a function of beam current and the system geometry.

1. INTRODUCTION

It is well known that the regimes in which an electron beam interacts with a plasma, and the efficient electromagnetic radiation that accompanies this interaction, are to a considerable extent determined by the beam current and the geometry of the plasma-beam structure.[1-3] From a practical point of view, beam-plasma structures of waveguiding type with transverse nonuniformity are especially promising, as indicated by the results of both theoretical[4,5] and experimental[5,6] papers on high-power plasma microwave oscillators based on relativistic electron beams. For this reason, the investigation of these devices has been pursued intensively in recent times.

In this paper we present a theoretical treatment of linear and nonlinear amplification of electromagnetic waves in a magnetized beam-plasma system of general form with transverse density variation. We give a detailed discussion of the case of cylindrical geometry, i.e., amplification in a circular waveguide containing a thin hollow beam and a plasma with the same structure, and show that five different amplification regimes are possible, depending on the geometry of the structure and on the beam current. This is in agreement with the results of Ref. 2, in which the analogous geometry was investigated in linear approximation in connection with the initial-value problem for the case of low frequencies. We identify the ranges of beam current and electromagnetic wave frequency for which the regime of maximum amplification is realized, and determine values of these parameters that bound the amplification range in the waveguide. Using analytical and numerical methods, we investigate the field amplitude, conversion efficiency for beam energy into radiation, and radiated electromagnetic power as a function of the magnitude of the beam current and geometry of the system. We also classify the nonlinear amplification regimes.

2. FUNDAMENTAL NONLINEAR EQUATIONS

Let us consider a metal waveguide of arbitrary cross-section containing a thin beam and a plasma. In setting up boundary conditions for the problem of amplification of oscillations fed to the input of such a waveguide, we describe the electromagnetic properties of the structure using the following system of equations:

$$\frac{\partial}{\partial z}\left(\Delta_\perp+\frac{\partial^2}{\partial z^2}-\frac{1}{c^2}\frac{\partial^2}{\partial t^2}\right)\psi=-4\pi(j_{pz}+j_{bz}),$$

$$\frac{dt}{dz}=\frac{1}{v_z},$$

$$v_z\frac{dv_z}{dz}=\frac{e}{m}\left(1-\frac{v_z^2}{c^2}\right)^{3/2}E_z,$$

$$\frac{\partial\tilde{j}_p}{\partial t}=\frac{\omega_p^2}{4\pi}E_z, \qquad (1)$$

$$E_z=\left(\frac{\partial^2}{\partial z^2}-\frac{1}{c^2}\frac{\partial^2}{\partial t^2}\right)\psi,$$

$$j_{bz}=en_bS_b\delta(\mathbf{r}_\perp-\mathbf{r}_b)\int v_z(z,t)\delta[t-t(z,t_0)]dt_0,$$

$$j_{pz}=S_p\delta(\mathbf{r}_\perp-\mathbf{r}_p)\tilde{j}_p.$$

Here $\mathbf{r}_\perp$ is the position in the transverse cross-section; $\mathbf{r}_b$ and $\mathbf{r}_p$ are the positions of the beam and plasma in the waveguide; S_b and S_p are the areas of their transverse cross-sections; $\Delta_\perp$ is the transverse part of the Laplacian operator; $\psi=\psi(z,t,\mathbf{r}_\perp)$ is the Hertz polarization potential;[7] $E_z=E_z(z,t,\mathbf{r}_\perp)$ is the longitudinal component of the electric field; and j_{bz} and j_{pz} are the perturbations of the beam and plasma currents respectively. In writing the system (1), we have assumed that the beam and plasma are completely magnetized by an external magnetic field directed along the z-axis.

For clarity, the first equation in system (1) is a result of transfer of Maxwell equations for the cylindrical magnetic waves of E-type. Next two equations are the characteristic system for Vlasov's equation, which describe an electron beam, and equation for $\tilde{j}_p$ is a result of linear equations for hydrodynamic for the plasma electrons. In general, system (1) is widely used for solving various problems in plasma and vacuum UHF electronics.[3,8] The polarization potential ψ and electric field E_z reduce to zero at the metallic wall of the waveguide, and satisfy the condition of periodicity in the coordinate t:

$$\psi(z,0,\mathbf{r}_\perp)=\psi(z,T,\mathbf{r}_\perp),\quad E_z(z,0,\mathbf{r}_\perp)=E_z(z,T,\mathbf{r}_\perp), \qquad (2)$$

where $T=2\pi/\omega$ is the period of the electromagnetic oscillations fed in at the waveguide input. The input of the waveguide corresponds to the coordinate $z=0$. Note that the plasma behavior implicit in Eqs. (1) corresponds to the linear approximation. The validity of this approach will be justified below.

It is known that the oscillations that are amplified most efficiently in a beam plasma waveguide are those with longitudinal wave numbers of order ω/u, where u is the velocity of the unperturbed beam. Then the Hertz polarization potential can be conveniently written in the form

 0038-5646/92/020242-11$05.00 © 1992 American Institute of Physics

$$\psi(z,t,\mathbf{r}_\perp)=\frac{1}{2}\sum_{n=1}^{\infty}\varphi_n(\mathbf{r}_\perp)\left[A_n(z)\exp\left(-i\omega t+i\frac{\omega}{u}z\right)+\text{c.c.}\right]. \tag{3}$$

Here, $A_n(z)$ is a slowly-varying function (i.e., the characteristic length scale over which A_n varies is smaller than u/ω), and ψ_n is a waveguide eigenfunction. We note that for transverse-nonuniform beam-plasma waveguides it is meaningful in principle to include all the terms of the infinite sum in (3). Therefore, in contrast to the usual approach in the theory of transverse-uniform systems,[3] in which one or several low-order terms of the series are taken into account, in this paper we will use an entirely different method. Let us briefly describe its essential features.

We first substitute the representation (3) into the first equation of the system (1). After multiplying the resulting expression by $\varphi_n(\mathbf{r}_\perp)$ and integrating it over the transverse cross-section of the waveguide, we find the coefficients A_n in the form

$$A_n=i\frac{4\pi}{\omega}\hat{D}_n\left[en_bu\frac{S_b}{S_w}\frac{\varphi_u(\mathbf{r}_b)}{\|\varphi_n\|^2}\rho_b+\frac{S_p}{S_w}\frac{\varphi_n(\mathbf{r}_p)}{\|\varphi_n\|^2}j_p\right], \tag{4}$$

where

$$\rho_b=\frac{2}{T}\int_0^T\frac{v_z}{u}\exp(i\omega t')dt_0,\quad j_p=\frac{2}{T}\int_0^T\tilde{j}_p\exp(i\omega t')dt'. \tag{5}$$

Here $t'=t-z/u$, S_w is the area of the transverse cross-section of the waveguide, $\|\varphi_n\|$ is the norm of the eigenfunction, and

$$\hat{D}_n=\left[k_{\perp n}^2+\frac{\omega^2}{u^2\gamma^2}\left(1-2i\gamma^2\frac{u}{\omega}\frac{d}{dz}\right)\right]^{-1} \tag{6}$$

is a pseudodifferential operator. Here, $\gamma=(1-u^2/c^2)^{-1/2}$, and $k_{\perp n}$ is the transverse wave number. Using the slow variation of A_n, let us expand $\hat{D}_n$ in a series with respect to d/dz, and save only the first term in the expansion. As a result, we have the following expression for the operator $\hat{D}_n$:

$$\hat{D}_n\approx\frac{1}{k_{\perp n}^2+\omega^2/u^2\gamma^2}\left(1+2i\frac{\omega}{u}\frac{1}{k_{\perp n}^2+\omega^2/u^2\gamma^2}\frac{d}{dz}\right), \tag{7}$$

which is valid under the following condition:

$$k_{\perp n}^2+\frac{\omega^2}{u^2\gamma^2}\gg 2\frac{\omega}{u}\left|\frac{d}{dz}\right|\sim 2\frac{\omega}{u}|\delta k_z|, \tag{8}$$

where δk_z is the amplification coefficient, or in other words the inverse characteristic length over which A_n changes. We note that inequality (8) is easily satisfied both for high-density and low-density beams, especially for frequencies that are not too high.

In order to obtain nonlinear equations, we now substitute (3) and (4) into the third and fourth equations of the system (1). Without taking time for some uncomplicated but tedious transformations, we immediately introduce the dimensionless variables

$$\xi=\frac{\omega}{u}z,\quad y=\omega t',\quad \eta=\frac{u-v_z}{u},\quad \sigma=2\gamma^2,$$
$$x=\frac{\omega R}{u\gamma},\quad \eta_0=\frac{1}{\sigma}\left(1-\frac{1}{\alpha_p}\right),\quad \tilde{\alpha}=\frac{G^2}{R_bR_p}, \tag{9}$$

$$\alpha_b=\frac{\omega_b^2R^2}{u^2\gamma^5}\frac{S_b}{S_w}R_b(x),\quad \alpha_p=\frac{\omega_p^2R^2}{u^2\gamma^2}\frac{S_p}{S_w}R_p(x),$$

$$R_j(x)=\sum_{n=1}^{\infty}\frac{1}{k_{\perp n}^2R^2+x^2}\frac{\varphi_n^2(\mathbf{r}_j)}{\|\varphi_n\|^2},\quad j=b,p,$$

$$G(x)=\sum_{n=1}^{\infty}\frac{1}{k_{\perp n}^2R^2+x^2}\frac{\varphi_n(\mathbf{r}_b)\varphi_n(\mathbf{r}_p)}{\|\varphi_n\|^2},$$
$$j_p=\alpha_p\frac{G}{R_p}\frac{j_p}{en_pu\gamma^3},$$

where R is a characteristic transverse size of the waveguide system, and write the transformed equations (1) in the following form:

$$\frac{dy}{d\xi}=\eta,$$
$$\frac{d\eta}{d\xi}=\frac{i}{2}(1+\sigma\eta)^{3/2}\left\{\alpha_be^{-iy}\left[1-i\sigma(1+f_b)\frac{d}{d\xi}\right]\rho_b+e^{-iy}\left[1-i\sigma(1+f_G)\frac{d}{d\xi}\right]j_p-\text{c.c.}\right\}. \tag{10}$$

$$\frac{dj_p}{d\xi}+i\frac{\eta_0}{1+f_p}j_p=-i\tilde{\alpha}\frac{\alpha_b}{\sigma}\frac{1}{1+f_p}\left[1-i\sigma(1+f_G)\frac{d}{d\xi}\right]\rho_b,$$
$$\rho_b=\frac{1}{\pi}\int_0^{2\pi}e^{iy}dy_0.$$

The quantity η_0 in Eqs. (10) has the sense of a detuning or deviation of the phase velocity of the plasma waves, which are as yet unperturbed by the beam, from the velocity u; the parameter α_b is proportional to the beam current, and $\tilde{\alpha}$ is the coupling parameter. If the positions of the beam and plasma coincide, then we have $\tilde{\alpha}=1$. When the beam and plasma are sufficiently far separated in space, we have $\tilde{\alpha}\to 0$.

The geometric factors R_b, R_p, and G [see (9)] have their origin in the zeroth-order terms of the expansion of the operator $\hat{D}_n$ (the number 1 in the curly brackets of Eq. (10) is a result of making these quantities dimensionless); their dependence on frequency ω (or x) is a consequence of the nonlinear dispersion law for the beam and plasma waves. The functions

$$f_j(x)=\frac{1}{2}x\frac{d\ln R_j}{dx},\quad j=b,p,\quad f_G(x)=\frac{1}{2}x\frac{d\ln G}{dx} \tag{11}$$

are a result of taking into account the next terms in the series expansion of the operator $\hat{D}_n$. In the low-frequency region f_b, f_p, and f_G all vanish.

The system of equations (10) contains all the necessary information on the electromagnetic processes in a waveguide structure with transverse variation. In this case, the Hertz polarization potential is completely determined by the eigenfunctions

$$\varepsilon(\xi,\mathbf{r}_1)=\sum_{n=1}^{\infty}\varepsilon_n(\xi)\varphi_n(\mathbf{r}_\perp),$$
$$\varepsilon_n=\frac{e}{m}\frac{\omega}{u^3}\gamma^{-5}A_n \tag{12}$$

and is given in terms of the perturbations of the charge density ρ_b of the beam and current density j_p of the plasma using Eqs. (4), (7):

$$\varepsilon(\xi, \mathbf{r}_\perp)=i\alpha_b\frac{\Phi_b}{R_b}\left(1-i\sigma\frac{1}{2}x\frac{d\ln\Phi_b}{dx}\frac{d}{d\xi}\right)\rho_b$$
$$+i\frac{\Phi_p}{G}\left(1-i\sigma\frac{1}{2}x\frac{d\ln\Phi_p}{dx}\frac{d}{d\xi}\right)j_p. \qquad (13)$$

Here

$$\Phi_j(\mathbf{r}_\perp, x)=\sum_{n=1}^{\infty}\frac{1}{k_{\perp n}^2R^2+x^2}\frac{\varphi_n(\mathbf{r}_\perp)\varphi_n(\mathbf{r}_j)}{\|\varphi_n\|^2}, \quad j=b,p. \qquad (14)$$

Note that the first term on the right side of the equation for η in the system (10) is the part of the force exerted on the beam electrons by the field of the beam's Langmuir waves; the second term, as will be clear below, includes both the rest of the force exerted by the beam waves and the force exerted by the field of the electromagnetic plasma waves. It is convenient to carry out an additional "separation" of the fields. To do this, we use the third equation of the system to eliminate the derivative $dj_p/d\xi$ and to rewrite the equation for η in the form

$$\frac{d\eta}{d\xi}=\frac{i}{2}(1+\sigma\eta)^{1/2}\left\{\alpha_b\left(1-\tilde{\alpha}\frac{1+f_G}{1+f_p}\right)\rho_b e^{-i\psi}\right.$$
$$-i\alpha_b\sigma\left[1+f_b-\tilde{\alpha}\frac{(1+f_G)^2}{1+f_p}\right]\frac{d\rho_b}{d\xi}e^{-i\psi}$$
$$\left.+\left(1-\sigma\eta_0\frac{1+f_G}{1+f_p}\right)j_p e^{-i\psi}-\text{c.c.}\right\}. \qquad (15)$$

As was shown in Ref. 3, the first and second terms on the right-hand side of the equation of motion (15) make up the total force exerted on the electron beam by the field of the beam Langmuir waves; the second term, which is due to the rotational nature of the beam wave, turns out to affect the amplification dynamics significantly only in the range of very high beam currents. Finally, the third term is the force exerted by the electromagnetic oscillations of the plasma. Incidentally, when the positions of the beam and plasma coincide ($\tilde{\alpha}=1, f_p=f_b=f_G$), the first two terms reduce to zero, and [as is clear from Eq. (15)] the third term acquires the meaning of a longitudinal electric field of the plasma waves, which are partially distorted due to the induced modulation of the beam density.

The system of equations (10) has a first integral. In order to find it we replace j_p by a new quantity j:

$$j_p=\left[1-i\sigma(1+f_G)\frac{d}{d\xi}\right]j. \qquad (16)$$

Since j_p is the amplitude of the longitudinal current perturbations in the plasma, it also determines the amplitude of the longitudinal component of the field E_z. Then the fifth equation of the system (1) implies that the quantity j from (16) gives the transverse component of the electromagnetic field, which determines the energy flux of the plasma waves. Taking into account (16), the first integral of the system (10) can be written in the form

$$\frac{1}{2\pi}\int_0^{2\pi}\frac{dy_0}{(1+\sigma\eta)^{1/2}}+\frac{1}{8}\alpha_b\sigma^2\left[1+f_b-\tilde{\alpha}\frac{(1+f_G)^2}{1+f_p}\right]|\rho_b|^2$$
$$+\frac{\sigma^2}{8}\frac{1+f_p}{\tilde{\alpha}\alpha_b}\left(1-\sigma\eta_0\frac{1+f_G}{1+f_p}\right)^2|j|^2=\text{const}, \qquad (17)$$

where the first term on the left side is the change in kinetic energy flux of the electrons in the beam, while the second and third terms are the fluxes of electromagnetic energy for the beam and plasma waves, respectively.

Let us begin with the worst case, and assume that the electromagnetic radiation can be emitted only from the plasma. Then the conversion efficiency of beam kinetic energy into energy of electromagnetic radiation is determined by the following expression:

$$K=\frac{\sigma^2}{8}\frac{1+f_p}{\tilde{\alpha}\alpha_b}\left(1-\sigma\eta_0\frac{1+f_G}{1+f_p}\right)^2(|j|^2-|j_0|^2), \qquad (18)$$

where $j_0=j|_{\xi=0}$.

3. CIRCULAR WAVEGUIDE WITH A THIN HOLLOW BEAM AND PLASMA

Let us consider a circular metallic waveguide of radius R, for which $\varphi_n=J_0(k_{\perp n}r)$ and $k_{\perp n}=\mu_{0n}/R$, where μ_{0n} are the roots of the zero-order Bessel function. Using the Knezer-Sommerfeld expression,[9] we evaluate the infinite sum in the geometric factors and write the quantities R_b and R_p, R_G, and α in explicit form:

$$R_j(x)=\frac{1}{2}I_0^2(xa_j)\left[\frac{K_0(xa_j)}{I_0(xa_j)}-\frac{K_0(x)}{I_0(x)}\right], \quad j=b,p, \qquad (19)$$

$$G(x)=\frac{1}{2}I_0(xa_b)I_0(xa_p)\begin{cases}\dfrac{K_0(xa_b)}{I_0(xa_b)}-\dfrac{K_0(x)}{I_0(x)}, & a_p\leqslant a_b,\\[2ex] \dfrac{K_0(xa_p)}{I_0(xa_p)}-\dfrac{K_0(x)}{I_0(x)}, & a_p\geqslant a_b,\end{cases}$$

$$\tilde{\alpha}=\begin{cases}\dfrac{K_0(xa_b)/I_0(xa_b)-K_0(x)/I_0(x)}{K_0(xa_p)/I_0(xa_p)-K_0(x)/I_0(x)}, & a_p\leqslant a_b,\\[2ex] \dfrac{K_0(xa_p)/I_0(xa_p)-K_0(x)/I_0(x)}{K_0(xa_b)/I_0(xa_b)-K_0(x)/I_0(x)}, & a_p\geqslant a_b,\end{cases} \qquad (20)$$

where I_0, K_0 are Bessel functions of imaginary argument, $a_b=r_b/R$, $a_p=r_p/R$, and r_b and r_p are radii of the thin hollow beam and plasma respectively. We also present the expressions for the coefficients Φ_b and Φ_p entering into Eq. 13, which determine the transverse structure of the field in the waveguide:

$$\Phi_j(a,x)=\frac{1}{2}I_0(xa)I_0(xa_j)\begin{cases}\dfrac{K_0(xa_j)}{I_0(xa_j)}-\dfrac{K_0(x)}{I_0(x)}, & a\leqslant a_j,\\[2ex] \dfrac{K_0(xa)}{I_0(xa)}-\dfrac{K_0(x)}{I_0(x)}. & a\geqslant a_j.\end{cases} \qquad (21)$$

Here $a=r/R$, while r is the coordinate in the transverse cross section of the waveguide.

The expressions for the functions f_b, f_p, f_G, and also for the derivatives of Φ_p and Φ_b with respect to x, are calculated

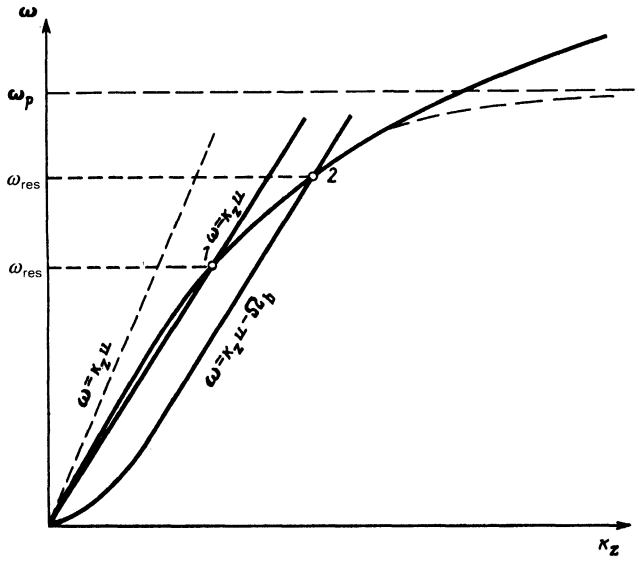

FIG. 1. Dispersion curves in the ω-k_z plane.

rather simply from Eqs. (19) and (21); however, due to their cumbersome form we do not present them here. As we already noted above, the functions f_j ($j = b,p,G$) vanish at low frequencies. As the frequency ω increases, the function f_b, e.g., increases monotonically in absolute value, and for large ω (or x) it goes to a value $f_b|_{x\to\infty} \to -0.5$. The functions f_p and f_G behave analogously. Thus, inclusion of the f_i does not cause any qualitative change in the process of beam-plasma interaction, and is important only quantitatively.

However, in a real system, for which the beam and plasma have finite thickness, we have $f_j \to -1$ as $\omega \to \omega_p$, which clearly leads to a qualitative change in the interaction dynamics. Let us pause to consider this question in detail, thereby addressing the question of how well a theory designed for an infinitely thin beam and plasma can describe a real system with a beam and plasma of finite thickness.

It is known that the only waves an infinitely thin plasma can support are surface waves, with a high-frequency dispersion law $\omega \sim (K_z)^{1/2}$ (similar to waves in deep water[10]). The corresponding dispersion law is shown in Fig. 1 by the solid curve. For the case of a plasma of finite width, the dispersion curve is asymptotic to the plasma frequency (the dot in Fig. 1) in this limit, and for $\omega \sim \omega_p$ the plasma oscillations turn out to be confined within the bulk of the finite-thickness plasma. Thus, there is a certain frequency at which the dispersion curve of an infinitely thin plasma begins to dive ge from that of a plasma of finite thickness, so that the theoretical results given above will not correspond to the real situation. However, if either of the resonance points 1 or 2 in Fig. 2 is located sufficiently far from the plasma frequency, i.e.,

$$\omega_{\rm res} \ll \omega_p, \tag{22}$$

this difference in dispersion curves will be unimportant.

The numerical analysis we carried out of the dispersion curves for a thin plasma and a plasma with finite thickness ($\Delta_p \simeq 1$ mm, $r_p = 0.9$ cm, $R = 1.8$ cm) shows that the dispersion curves at points 1 and 2 agree completely on an interval of plasma frequencies from $10\cdot 10^{10}$ sec^{-1} to $50\cdot 10^{10}$ sec^{-1} with $\gamma = 2$, and inequality (22) is satisfied. We note only that if $\omega_{\rm res} \sim \omega_p$, the field of the plasma oscillations is irrotational, and as we have already said, is completely "sealed" inside the plasma volume. This important change in the structure of the field is why we have $f_j \to -1$, and leads to the disappearance of the rotational (radiative) terms in Eq. (10). This latter phenomenon in turn has a deleterious effect on the amplification; therefore, fulfillment of inequality (22) is a strict necessity.

We have already noted that the theory constructed here treats the plasma in the linear approximation. Linear response of the plasma implies in turn that the plasma electron displacements in the longitudinal electric field are much smaller than the wavelength,[3] i.e.,

$$\lambda_p = \left| \frac{eEz}{k_z m u^2} \right| \ll 1. \tag{23}$$

Assuming $k_z = \omega/u$, and using the dimensionless variables (9), let us write the criterion for linearity in the circular waveguide as follows:

$$\lambda_p = \frac{u^2\gamma^5}{\omega_p^2 r_p \Delta_p} |j_p|_{max} \begin{cases} \left(\ln \dfrac{r_b}{R}\right)^{-1}, & r_p < r_b, \\ \left(\ln \dfrac{r_p}{R}\right)^{-1}, & r_p \geqslant r_b. \end{cases} \tag{24}$$

Specific values of λ_p for various amplification regimes are listed in Table II.

For further analysis of Eq. (10), the parameter α_b, which plays a significant role in determining the amplification mechanism, is conveniently expressed in terms of the ratio of the beam current j_b to the limiting vacuum current j_0 of a thin hollow beam (Ref. 3):

$$\alpha_b = \frac{J_b}{J_0} \gamma^{-2} \left(\frac{\gamma^{2/3}-1}{\gamma^2-1} \right)^{3/2} \frac{R_b(x)}{R_b(0)}. \tag{25}$$

For $x \ll 1$ and large γ, we have $\alpha_b \approx \gamma^{-4} J_b/J_0$.

4. LINEAR THEORY

In the linear approximation, when we have $j_p \propto \exp(i\delta k_z z)$, it is easy to obtain the following dispersion equation from the system (10):

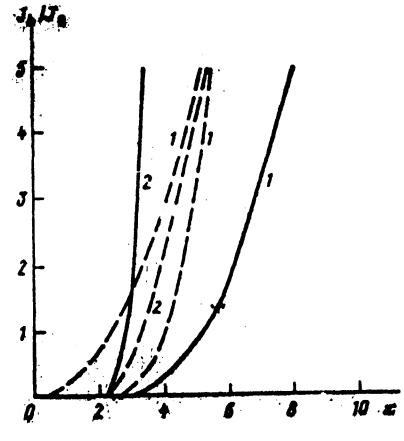

FIG. 2. Curve for cutoff (1) and curve for maximum amplification (2) when $a_b = 0.5$ (solid) and 0.8 (dashed); $\omega_p = 25\cdot 10^{10}$ sec^{-1}.

$$\{\delta^2-\alpha_b[1+(1+f_b)\sigma\delta]\}[(1+f_p)\delta+\eta_0]$$

$$=-\tilde{\alpha}\frac{\alpha_b}{\sigma}[1+(1+f_G)\sigma\delta]^2, \qquad (26)$$

where $\delta = (u/\omega)\delta k_z$ is the dimensionless amplification coefficient. Note that in the low-frequency limit, where f_b, f_p, and f_G are absent, an analogous dispersion equation was obtained and analyzed in Ref. 2.

For further analysis, we rewrite the dispersion relation (26) in the form

$$(\delta-\delta_1)(\delta-\delta_2)[(1+f_p)\delta+\eta_0]=-\tilde{\alpha}\frac{\alpha_b}{\sigma}[1+(1+f_G)\sigma\delta]^2, \qquad (27)$$

where the quantity

$$\delta_{1,2}={}^1/_2\alpha_b\sigma(1+f_b)\pm{}^1/_2[\alpha_b^2\sigma^2(1+f_b)^2+4\alpha_b]^{1/2} \qquad (28)$$

determines the spectrum of slow and fast beam waves; in the boundary value problem, the sign " + " corresponds to a slow wave. Let us investigate further the two types of resonance that are of most interest. The first is characterized by interactions of the wave-particle type, and takes place for $v_{\rm ph} = u$ (see point 1 on Fig. 1), where $v_{\rm ph}$ is the phase velocity of the plasma wave. In the variables (9) this corresponds to a detuning $\eta_0 = 0$. The second is characterized by a wave-wave type of interaction, and takes place for $v_{\rm ph} = v_b$ (point 2 in Fig. 1), where v_b is the phase velocity of the slow beam wave; in the variables (9) this corresponds to $\eta_0 = -\delta_1$.

Depending on the beam current J_b, the coupling parameter $\tilde{\alpha}$, and the corresponding resonance condition (Fig. 1), five different regimes are possible for the amplification of oscillations in a waveguide with a thin hollow beam and plasma.[2] In the limiting cases of low-current ($J_b \ll J_0$) and high-current ($J_b \gg J_0$) beams, and also depending on the mutual positions of the plasma and the beam ($\tilde{\alpha}\sim 1$ or $\tilde{\alpha}\ll 1$), the amplification coefficient can be explicitly found in the form of simple analytic expressions,[2] and is represented in the upper rows of Table I.

For intermediate values of the current and coupling parameter $\tilde{\alpha}$, the solution to the dispersion relation has a rather cumbersome form, and is conveniently analyzed numerically. We will carry out this analysis starting from the parameters of a real experiment:[11] $\gamma = 2$ ($\sigma = 8$); $R = 1.8$ cm, $r_p = 0.9$ ($a_p = 0.5$). We will vary the plasma frequency and the position of the beam a_b.

In Fig. 2 we show a curve of maximum amplification in the variables (J_b/J_0), x, and the curve for cutoff of the amplification[1)] when $\omega_p = 25\cdot 10^{10}\,\text{sec}^{-1}$. The solid curves correspond to $a_b = 0.5$, where the radii of the beam and plasma coincide ($\tilde{\alpha} = 1$); curve 1 is the curve for cutoff (the amplification region is located to the left), while curve 2 is the curve for maximum amplification of the oscillations. For $a_b = 0.8$, when the beam and plasma are separated in space, the region of amplification is bounded with respect to frequency, both above (on the right in Fig. 2) and below (on the left in Fig. 2; see dotted curve No. 1 in Fig. 2) and the maximum amplification occurs roughly in the center of the diagram (the dotted curve 2). The bounding of the region of amplification with frequency above and below is explained by the topology of the dispersion curves, whose qualitative form is shown in Ref. 2. We note that for $r_b < r_p$ (here we investigate the case $a_b = 0.2$), the curves for cutoff of the amplification have an analogous form, and therefore will not be shown here.

As the plasma frequency increases, the cutoff and maximum-amplification curves shift to the right. In this case, for $a_b = 0.8$ the region of amplification becomes narrower with respect to frequency. Thus, for $\omega_p = 25\cdot 10^{10}\,\text{sec}^{-1}$, we have $J_b/J_0 \sim 1$, $\Delta x = x_{\max} - x_{\min} \sim 1.6$, and $|\text{Im}\delta|_{\max} \sim 0.05$; for $\omega_p = 35\cdot 10^{10}\,\text{sec}^{-1}$ we have $J_b/J_0 \sim 1$, $\Delta x \sim 0.75$, and $|\text{Im}\delta|_{\max} \sim 0.013$; for $\omega_p = 50\cdot 10^{10}\,\text{sec}^{-1}$ we have $J_b/J_0 \sim 1$, $\Delta x \sim 0.25$, and $|\text{Im}\delta|_{\max} \sim 0.002$. This is explained by the fact that the value of the resonance frequency $\omega_{\rm res}$ increases with increasing plasma frequency ω_p as well (points 1 and 2 in Fig. 1 are displaced upward). Consequently, the coupling coefficient $\tilde{\alpha}$ becomes exponentially small, the region of amplification contracts, and the amplification coefficient decreases.

Conversely, for $a_b = 0.5$ there is no lower frequency limit for amplification (more precisely, it is given by the expression $x = 0$); therefore the region of amplification increases with increasing ω_p, and amplification of electromagnetic signals with rather wide frequency bandwidths becomes possible.

An interesting situation arises as the plasma frequency decreases. For example, at $\omega_p = 10\cdot 10^{10}\,\text{sec}^{-1}$ the straight line $\omega = k_z u$ no longer crosses the curve for characteristic plasma oscillations in the ω, k_z plane (see the dotted curve $\omega = k_z u$ in Fig. 1). In this case, only the curve $\omega = k_z u - \Omega_b$ ($\Omega_b = x\alpha_b$), which describes the spectrum of slow beam waves, participates in the "coupling" of the dispersion curves. In reality, this "coupling" does occur for sufficiently dense beams, or starting with a certain threshold current. This fact is well-confirmed by Fig. 3, where we show the curve for cutoff of amplification when $\omega_p = 10\cdot 10^{10}\,\text{sec}^{-1}$ (the solid curve corresponds to $a_b = 0.5$, the dotted curve to $a_b = 0.8$). For a beam and plasma that are separated in space ($a_b = 0.8$), there is a frequency bound on the range of amplification from below in this case as well; however, this boundary exists only for values of the current $J_b/J_0 > 5$, and therefore does not appear in Fig. 3. We note that this current threshold for the regime of plasma wave amplification was treated in Ref. 12 for the case of a transversely uniform beam-plasma waveguide.

5. NONLINEAR AMPLIFICATION DYNAMICS IN A WAVEGUIDE

The system of nonlinear equations (15) was analyzed numerically for the following boundary conditions:

$$y|_{\xi=0}=y_0\in[0,2\pi],\quad \eta|_{\xi=0}=0\quad j_p|_{\xi=0}=j_{p0}=10^{-4} \qquad (29)$$

and the following values of the fixed parameters: $\gamma = 2$ ($\sigma = 8$), $r_p = 0.9$ ($a_p = 0.5$), $R = 1.8$ cm, $\omega_p = 25\cdot 10^{10}\,\text{sec}^{-1}$, and $\omega = 7.78\cdot 10^{10}\,\text{sec}^{-1}$ ($x = 2.7$), which correspond to a real experimental situation.[11] In this case, the remaining free parameters are the quantities a_b and J_b/J_0.

Let us analyze how nonlinear stabilization of the five different amplification mechanisms comes about as a function of the beam current, its position, and the resonance conditions corresponding to Table I. In the following section, some of the regimes listed in the table will be investigated analytically.

TABLE I.

		$\eta_0 = 0\ (v_\Phi = u)$	$\eta_0 = -\delta_1\ (v_\Phi = v_b)$
$J_b \ll J_0$ $(\alpha_b\sigma^2 \ll 1)$	$\tilde{\alpha} \sim 1$	$\delta = \frac{1 - i\cdot 3^{1/2}}{2}\left(\tilde{\alpha}\frac{\alpha_b}{\sigma}\frac{1}{1+f_p}\right)^{1/3}$, $\lvert\rho\rvert_{max} \sim 1$, $\lvert j\rvert_{max} \sim \left(\tilde{\alpha}\frac{\alpha_b}{\sigma}\right)^{2/3}$, $K_{max} \sim (\alpha_b\sigma^2)^{1/3} \sim J_b^{1/3}$ 1.1	$\delta = \frac{1 - i\cdot 3^{1/2}}{2}\left(\tilde{\alpha}\frac{\alpha_b}{\sigma}\frac{1}{1+f_p}\right)^{1/3}$, $\lvert\rho\rvert_{max} \sim 1$, $\lvert j\rvert_{max} \sim \left(\tilde{\alpha}\frac{\alpha_b}{\sigma}\right)^{2/3}$, $K_{max} \sim (\alpha_b\sigma^2)^{2/3} \sim J_b^{1/3}$ 1.2
	$\tilde{\alpha} \sim 0$	Stability 1.3	$\delta = -i\left(\tilde{\alpha}\frac{\alpha_b^{1/2}}{2\sigma}\frac{1}{1+f_p}\right)^{1/2}$, $\lvert\rho\rvert_{max} = 2\left(\frac{2\tilde{\alpha}}{\sigma\alpha_b^{1/2}}\right)^{1/4}$, $\lvert j\rvert_{max} = 2\left(2\cdot 2^{1/2}\frac{\tilde{\alpha}^{3/2}\alpha_b^{3/4}}{\sigma^{3/2}}\right)^{1/2}$ $K_{max} = (2\tilde{\alpha}\alpha_b^{1/2}\sigma)^{1/2} \sim J_b^{1/4}$ 1.4
$J_b \gg J_0$ $(\alpha_b\sigma^2 \gg 1)$	$\tilde{\alpha} \sim 1$	$\delta = -i\alpha_b^{1/2}$ $\lvert j\rvert_{max} \approx \frac{2}{\sigma^2}$ $K_{max} \approx \frac{1}{2\alpha_b\sigma^2} \sim J_b^{-1}$ 1.5	$\delta = \frac{1}{2}\tilde{\alpha}\alpha_b\sigma\frac{(1+f_G)^2}{1+f_p}\left[1 - i\left(\frac{4}{\tilde{\alpha}}\frac{(1+f_b)(1+f_p)}{(1+f_G)^2} - 1\right)^{1/2}\right]$, $\lvert j\rvert_{max} \approx \frac{2}{\alpha_b\sigma^4}$, $K_{max} \approx \frac{1}{2\alpha_b\sigma^2} \sim J_b^{-1}$ 1.6
	$\tilde{\alpha} \sim 0$	Stability 1.7	$\delta = -i\tilde{\alpha}^{1/2}\alpha_b\sigma\left(\frac{1+f_b}{1+f_p}\right)^{1/2}(1+f_G)$, $\lvert\rho\rvert_{max} = 4\cdot\left(\frac{2}{3}\right)^{1/2}\frac{\tilde{\alpha}^{1/4}}{\alpha_b\sigma^2}$, $\lvert j\rvert_{max} = 4\cdot\left(\frac{2}{3}\right)^{1/2}\frac{\tilde{\alpha}^{3/4}}{\alpha_b\sigma^4}$, $K_{max} = \frac{4}{3}\frac{\tilde{\alpha}^{1/2}}{\alpha_b\sigma^2} \sim J_b^{-1}$ 1.8

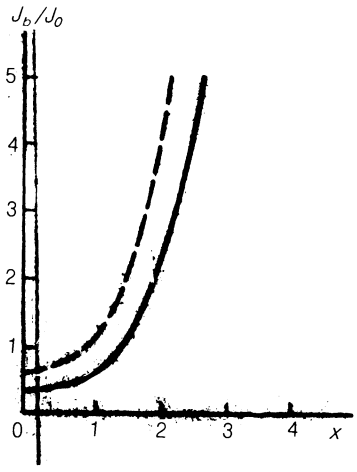

FIG. 3. Curve for cutoff of amplification when $a_b = 0.5$ (solid curve) and 0.8 (dashed curve), for $\omega_p = 10 \cdot 10^{10}$ sec^{-1}.

Let us consider the case of a low-current beam with $I_b = 0.1$ (where $I_b = J_b/J_0$). If the positions of the beam and plasma coincide, i.e., $a_b = 0.5$, so that $\tilde{\alpha} = 1$, then the single-particle Cherenkov effect occurs regardless of the resonance conditions,[13] as stated in columns 1.1 and 1.2 of Table I. In this case, the quantities $|j_p|$ and $|j|$ are the same order of magnitude; after saturation they exhibit quite regular oscillations, a characteristic of the well-known mechanism of nonlinear stabilization, i.e., trapping of beam electrons by the plasma wave field.[14]

When the beam and plasma are separated in space ($a_b = 0.8$ and $\tilde{\alpha} \simeq 0.15$), the region of zero detuning ($\eta_0 = 0$) lies outside the amplification region (see Fig. 2 and column 1.3 of Table I). Stability is possible for $\eta_0 \approx -\delta_1$ (column 1.4 in Table I), and exact equality implies a regime of maximum amplification. The characteristic behavior of $|j_p|$ and $|j|$ (less regular oscillation after saturation) and the electrons becoming turbulent in the phase plane is indicative of amplification taking place in the regime of the collective Cherenkov effect; here the nonlinear stabilization is also determined by a well-known mechanism, i.e., trapping of the electrons by the field of the slow beam wave,[3] i.e., "breaking" of the latter.

Let us turn to a discussion of the high-current electron beam. For the case $a_b = 0.5$ ($\tilde{\alpha} = 1$), and a beam current that varies between $I_b = 2$ and $I_b = 5$ (column 1.5 in Table I), there is a sharp decrease in the quantity $|j|$, which determines the transverse component of the field, compared to $|j_p|$. The latter is explained by the restructuring of the polarization of the plasma waves[15] and conversion of the radiative regime to a nonradiative regime, for which the instability is of the well-known "negative mass" type[3] and is characteristic of a medium with negative dielectric permittivity. The primary fraction of beam kinetic energy in this case goes into excitation of longitudinal potential oscillations in the beam, which explains the decrease in the conversion efficiency of

TABLE II.

	J_b/J_0	0,1	0,5	1	1,2	2
a_b=0,2						
(r_b=0,36 cm)	z_{max}, cm	61	45	45	38	53
	P_0, kW	23	23	23	23	23
	P_{max}, MW	27	141	274	101	32
	P_b, GW	0,12	0,6	1,2	1,8	2,4
J_0=2,38 kA	K_{max}	0,22	0,235	0,228	0,056	0,0135
	λ_p	0,02	0,05	0,07	0,04	0,03
	J_b/J_0	0,1	0,5	1	2	5
a_b=0,5						
(r_b=0,9 cm)	z_{max}, cm	29	17	14	11	8
	P_0, kW	12	12	12	12	12
	P_{max}, MW	72	307	535	874	1512
	P_b, GW	0,28	1,4	2,8	5,6	14
J_0=5,52 kA	K_{max}	0,26	0,22	0,19	0,156	0,11
	λ_p	0,05	0,13	0.18	0,32	0,5
	J_b/J_0	0,1	0,5	1	2	5
a_b=0,65						
(r_b=1,17 cm)	z_{max}, cm	42	27	23	22	18
	P_0, kW	40	40	40	40	40
	P_{max}, MW	108	458	935	1989	875
	P_b, GW	0,444	2,22	4,44	8,88	22,2
J_0=8,88 kA	K_{max}	0,24	0,206	0,21	0,22	0,04
	λ_p	0,05	0,11	0,17	0,26	0,24
	J_b/J_0	0,1	0,5	1	2 (x=3,9)	3 (x=4,5)
a_b=0,8						
(r_b=1,44 cm)	z_{max}, cm	63	52	48	28	30
	P_0, kW	180	180	180	345	500
	P_{max}, MW	198	1333	337	888	862
	P_b, GW	0,86	4,3	8,6	17,2	25,8
J_0=17.2 kA	K_{max}	0,23	0,31	0,04	0,05	0,033
	λ_p	0,06	0,16	0,09	0,09	0,07

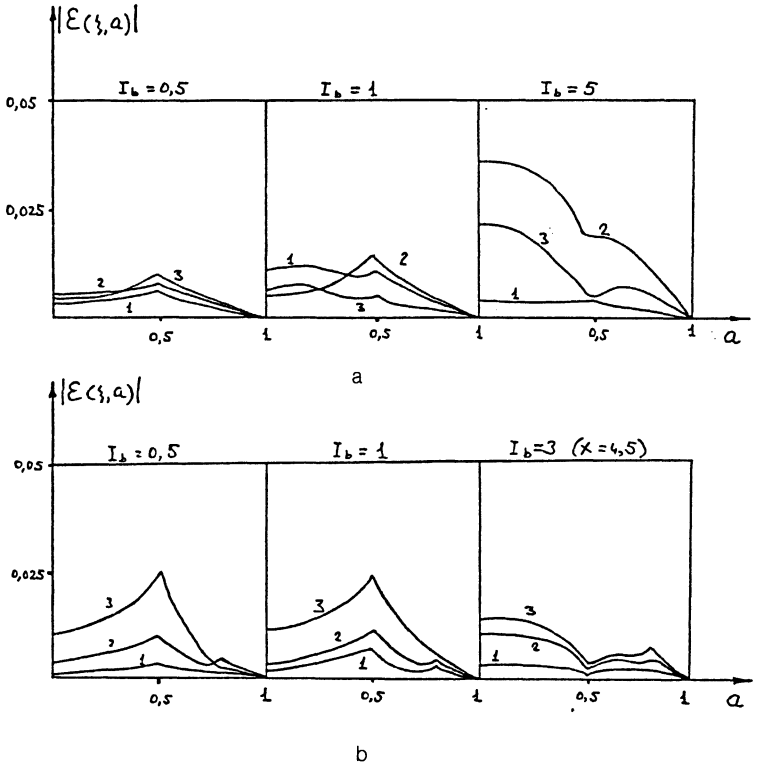

a

b

FIG. 4. Transverse structure of waveguide field. a—$a_b = 0.5$: $I_b = 0.5$ [$\xi = 40$ (*1*), 60 (*2*), 100 (*3*)]; $I_b = 1$ [$\xi = 40$ (*1*), 80 (*2*), 140 (*3*)], $I_b = 5$ [$\xi = 150$ (*1*), 250 (*2*), 400 (*3*)]; b—$a_b = 0.8$: $I_b = 0.5$ [$\xi = 50$ (*1*), 100 (*2*), 150 (*3*)]; $I_b = 1$ [$\xi = 100$ (*1*), 150 (*2*), 350 (*3*)], $I_b = 3$ [$x = 4.5$, $\xi = 80$ (*1*), 120 (*2*), 160 (*3*)]

beam energy into energy of radiation. The latter is quite apparent from Table II. In Fig. 4a we show the dynamics of the transverse structure of the electromagnetic field in the waveguide (see Eq. 13) for $a_b = 0.5$ and various values of the beam current.

The case where both amplification mechanisms, i.e., the negative-mass and collective Cherenkov regimes, are realized is well illustrated in Fig. 5, which shows the spatial dynamics of the quantities $|j_p|$ and $|j|$ for $a_b = 0.65$ and $I_b = 5$ (column 1.6 in Table I). In the high-current regime, it is the relativistic collective Cherenkov effect that is responsible for the "soliton-like" behavior of $|j_p|$ and $|j|$; the fact that $|j_p|$ exceeds $|j|$ by more than a factor of two is an indication that the system is operating in the negative-mass regime as well.

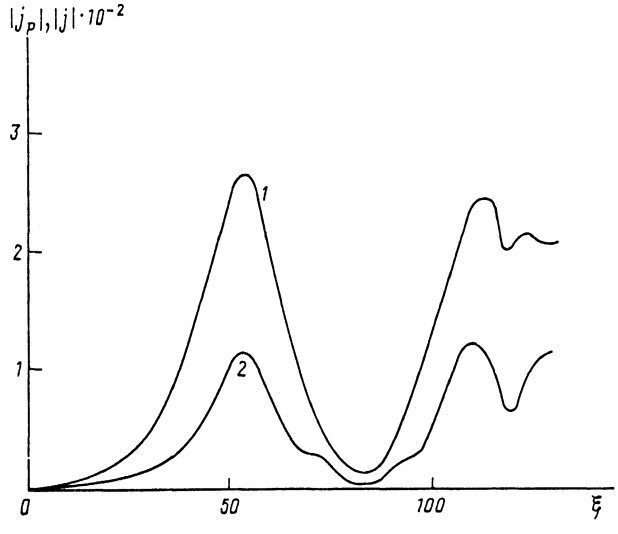

FIG. 5. Spatial dynamics of the quantities $|j_p|$ (1) and $|j|$ (2) for $a_b = 0.65$ and $I_b = 5$.

Finally, for $a_b = 0.8$ ($\tilde{a} \approx 0.06$), the mechanism that operates in the high-current region is the relativistic collective Cherenkov effect (column 1.8 in Table I). The soliton-like character of the solution is easy to see in Fig. 6, where we show the spatial dynamics of the quantities $|j_p|$ and $|j|$ for $I_b = 3$. In contrast to the previous case, here we have $|j_p| \lesssim |j|$, which is characteristic of the purely radiative regime. This solution was first obtained in Ref. 16 for the example of a simpler beam-plasma structure. We note that our numerical investigation of this latter case was for $x = 4.5$, corresponding to maximum amplification, since, as is clear from Fig. 2, there is a zone of stability at frequency $x = 2.7$ for currents $I_b \gtrsim 1.2$. The dynamics of the transverse structure of the field at $a_b = 0.8$ are shown in Fig. 4b for various values of the beam current.

More detailed results of our numerical calculations as a function of radius and beam current are listed in Table II. Here $z_{\max}$ is the optimum amplification length, P_0 and $P_{\max}$ are the input and output electromagnetic radiative powers, respectively ($P_{\max} = P|_{z=z\max}$), P_b is the beam power, $K_{\max}$ is the maximum conversion efficiency of beam energy into electromagnetic radiative energy, and λ_p is the linearity parameter of the plasma. We remind the reader that these calculations were carried out for values of the fixed parameters given above, with the exception of the two latter cases in the low-frequency part of the table, where the value of the frequency x is specified separately. We also note that the sharp decreases in the energy conversion efficiency $K_{\max}$ for $a_b = 0.2$, $I_b = 2$, and $a_b = 0.8$, $I_b = 1.0$, are due to the closeness of these points to the curve for cutoff of the amplification.

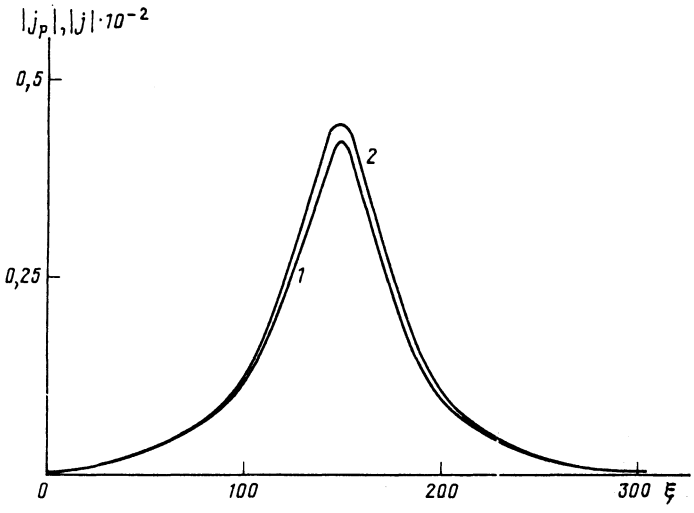

FIG. 6. Spatial dynamics of the quantities $|j_p|$ (1) and $|j|$ (2) for $a_b = 0.8$ and $I_b = 3$.

6. COORDINATE AND MOMENTUM EXPANSIONS IN THE THEORY OF TRANSVERSE-NONUNIFORM AMPLIFIERS

It is known that in the regimes where the "negative-mass" and "collective Cherenkov" types of instabilities are present (for both the high-current and low-current regimes) the nonlinear plasma-beam interaction can be treated analytically.[16,17] Using the methods we developed in Refs. 17, 18, i.e., expanding along the trajectories and momenta of the electrons, we give a similar analytic treatment here.

Let us introduce the electron momentum

$$p=(1+\sigma\eta)^{-1/2} \tag{30}$$

Using Eq. (16), we rewrite Eq. (10) in the form

$$\begin{gathered}\frac{dy}{d\xi}=\frac{1}{\sigma}\left(\frac{1}{p^2}-1\right),\\ \frac{dp}{d\xi}=-\frac{i}{4}\sigma\Big[\alpha_b(1-2\tilde{\alpha}+\tilde{\alpha}\sigma\eta_0)\rho_b e^{-iy}-i\alpha_b\sigma(1-\tilde{\alpha})\frac{d\rho_b}{d\xi}e^{-iy}\\ +(1-\sigma\eta_0)^2 j e^{-iy}-\text{c.c.}\Big],\\ \frac{dj}{d\xi}+i\eta_0 j=-i\tilde{\alpha}\frac{\alpha_b}{\sigma}\rho_b,\\ \rho_b=\frac{1}{\pi}\int_0^{2\pi}e^{iy}\,dy_0.\end{gathered} \tag{31}$$

In Eqs. (31), for simplicity in later expressions we discard the functions f_b, f_p, and f_G, which, as we mentioned above, give only rather small quantitative corrections.

We write the coordinates and momentum of an electron in the form[16,17]

$$\begin{gathered}y=y_0+W(\xi)+\tilde{y}(\xi,\,y_0),\quad |\tilde{y}|\ll 1,\\ p=\langle p\rangle_{(\xi)}+{}^1/_2(a(\xi)\exp(-iy_0)+\text{c.c.}),\end{gathered} \tag{32}$$

where $W(\xi)$ describes the constant displacement of an electron, $\tilde{y}$ its oscillations, $\langle p\rangle$ the average momentum, and $a(\xi)$ the momentum oscillations. Substituting the representation (32) into the system (31) and integrating over y_0 using the theory of residues, we obtain the following system of equations:

$$\begin{gathered}\frac{dW}{d\xi}=-\frac{1}{\sigma}\left[1-\frac{\langle p\rangle}{(\langle p\rangle^2-\sigma^2|A|^2)^{3/2}}\right],\\ \frac{d\rho}{d\xi}=-2i\frac{A}{(\langle p\rangle^2-\sigma^2|A|^2)^{3/2}},\\ \frac{dA}{d\xi}=-\frac{i}{2}\alpha_b(1-2\tilde{\alpha}+\tilde{\alpha}\sigma\eta_0)\rho_b e^{-iW}-\frac{1}{2}\alpha_b\sigma(1-\tilde{\alpha})\frac{d\rho_b}{d\xi}e^{-iW}\\ -\frac{i}{2}(1-\sigma\eta_0)^2 j e^{iW},\\ \frac{dj}{d\xi}+i\eta_0 j=-i\tilde{\alpha}\frac{\alpha_b}{\sigma}\rho_b,\\ \langle p\rangle=1-\frac{\sigma^2}{8}\left[\alpha_b(1-\tilde{\alpha})|\rho_b|^2+\frac{(1-\sigma\eta_0)^2}{\tilde{\alpha}\alpha_b}(|j|^2-|j_0|^2)\right],\\ \rho_b=\rho e^{iW}.\end{gathered} \tag{33}$$

Here $A = a/\sigma$.

Let us consider the amplification regime for which $J_b \gg J_0$ $(a_b\sigma^2 \gg 1)$, $\tilde{\alpha} = 1$, and $\eta_0 = 0$ (column 1.5 in Table I), where a "negative-mass" type of stabilization mechanism is realized. In this case, the overall slowing of the beam is unimportant ($W = 0$) and the stabilization mechanism is determined by complete modulation of the relativistic beam with respect to momentum.[3] The system of equations (33) simplifies considerably, and has the form

$$\begin{gathered}\frac{d\rho}{d\xi}=-2i\frac{A}{(\langle p\rangle^2-\sigma^2|A|^2)^{3/2}},\\ \frac{dA}{d\xi}=\frac{i}{2}\alpha_b\rho-\frac{i}{2}j,\\ \frac{dj}{d\xi}=-i\frac{\alpha_b}{\sigma}\rho.\end{gathered} \tag{34}$$

Eliminating ρ from the last two equations and assuming $\sigma dj/d\xi \gg j$, since $\sigma|d/d\xi| \sim \sigma|\delta| = \sigma\alpha_b{}^{1/2} \gg 1$, we have

$$A=-{}^1/_2\sigma j. \tag{35}$$

The electron beam is completely modulated in momentum when the denominator in the first term of system (34) vanishes i.e., $\alpha|A|_{\max} = \langle p\rangle \approx 1$. From this we have the following expression for the maximum current amplitude

$$|j|_{max} \approx \frac{2}{\sigma^2} \tag{36}$$

and an expression for the conversion efficiency of beam energy into radiative energy

$$K_{max} \approx \frac{1}{2\alpha_b\sigma^2} \approx 0{,}2\,\frac{R_b(0)}{R_b(x)}\,\frac{J_0}{J_b}. \tag{37}$$

Thus, e.g., for $I_b = 5$ we have $K_{\max} \simeq 0.08$, whereas the results of numerical calculations as shown in Table II give $K_{\max} \simeq 0.1$.

For the case where the negative-mass regime coexists with the collective Cherenkov regime (column 1.6 in Table I) and, as before, $j_b \gg j_0$, we have $\tilde{\alpha} \approx 1$, but $\eta_0 = -\delta_1 \approx -\alpha_b\sigma$ [see Eq. (28)]. In this case, Eq. (33) goes over to the form

$$\begin{gathered}\frac{d\rho}{d\xi} = -2i\frac{A}{(\langle p\rangle^2-\sigma^2|A|^2)^{3/2}},\\ \frac{dA}{d\xi} = \frac{i}{2}\alpha_b^2\sigma^2\rho - \frac{i}{2}\alpha_b^2\sigma^4 j,\\ \frac{dj}{d\xi} - i\alpha_b\sigma j = -i\frac{\alpha_b}{\sigma}\rho\end{gathered} \tag{38}$$

and has the following solution for the maximum current amplitude $|j|_{\max}$ and energy conversion efficiency $K_{\max}$:

$$|j|_{max} \approx \frac{2}{\alpha_b\sigma^4}, \qquad K_{max} \approx \frac{1}{2\alpha_b\sigma^2}. \tag{39}$$

Let us now discuss the nonlinear theory of amplification in the "collective Cherenkov" regime, where the coupling parameter is

$$\tilde{\alpha} \ll 1. \tag{40}$$

In this case, the nonlinear stabilization is determined by two effects: overall braking of the beam, and the relativistic dependence of the plasma oscillations of the electron beam on their amplitude.[18] The first mechanism is decisive for a low-current beam ($J_b \ll J_0$), while the second dominates for a high-current beam ($J_b \gg J_0$). Both saturation mechanisms are lumped together under the general term "nonlinear frequency shift,"[19] and are described mathematically by cubic nonlinearities.

Expanding the denominators in the first two equations of the system (33) through cubic terms, and taking into account the inequality (40), we obtain the following system of nonlinear equations:

$$\begin{gathered}\frac{dW}{d\xi} = \frac{\sigma}{4}\left[\alpha_b|\rho_b|^2 + \frac{(1-\sigma\eta_0)^2}{\tilde{\alpha}\alpha_b}(|j|^2-|j_0|^2)+6|A|^2\right],\\ \frac{d\rho}{d\xi} = -2i\left[1+\frac{3}{8}\alpha_b\sigma^2|\rho_b|^2 + \frac{3}{8}\sigma^2\frac{(1-\sigma\eta_0)^2}{\tilde{\alpha}\alpha_b}(|j|^2-|j_b|^2)+\frac{3}{2}\sigma^2|A|^2\right]A,\\ \frac{dA}{d\xi} = -\frac{i}{2}\alpha_b\left(\rho_b - i\sigma\frac{d\rho_b}{d\xi}\right)e^{-iW} - \frac{i}{2}(1-\sigma\eta_0)^2 j e^{-iW},\\ \frac{dj}{d\xi} + i\eta_0 j = -i\tilde{\alpha}\frac{\alpha_b}{\sigma}\rho_b, \qquad \rho_b = \rho e^{iW}.\end{gathered} \tag{41}$$

For the case of a low-current beam (column 1.4 in Table I) when $j_b \ll j_0$ ($\alpha_b\sigma^2 \ll 1$, $\eta_0 \approx -\alpha_b^{1/2}$) the saturation is determined by the overall slowing of the electron beam, and Eq. (41) reduces to the form

$$\begin{gathered}\frac{d\rho}{d\xi} - \frac{i}{2}\alpha_b^{1/2}|\rho|^2\rho = \frac{i}{2\alpha_b^{1/2}}j,\\ \frac{dj}{d\xi} = -i\tilde{\alpha}\frac{\alpha_b}{\sigma}\rho.\end{gathered} \tag{42}$$

The solution to the system of equations (42) can be written in terms of elliptic functions, and has the form ($j = |j|, \rho = |\rho|$):

$$j^2 = \frac{j_{max}^2}{1+(j_{max}^2/j_0)\mathrm{cn}^2(y,r)}, \qquad \rho^2 = \rho_{max}^2\frac{\mathrm{sn}^2(y,r)}{1+(j_{max}^2/j_0^2)\mathrm{cn}^2(y,r)}, \tag{43}$$

$$\begin{gathered}j_{max} = 2\left(2^{3/2}\frac{\tilde{\alpha}^{3/2}\alpha_b^{5/4}}{\sigma^{3/2}}\right), \qquad \rho_{max} = 2\left(\frac{2\tilde{\alpha}}{\sigma\alpha_b^{1/2}}\right)^{1/4},\\ y = \left(\frac{\tilde{\alpha}\alpha_b^{1/2}}{2\sigma}\right)^{1/2}\xi, \qquad r = 1-\frac{j_0^2}{j_{max}^2},\end{gathered} \tag{44}$$

and the amplification length over which a maximum of j and ρ is reached is determined by the expression

$$\xi_0 = \left(\frac{2\sigma}{\tilde{\alpha}\alpha_b^{1/2}}\right)^{1/2}\ln\left(2^{3/2}\frac{j_{max}}{j_0}\right). \tag{45}$$

The maximum energy conversion efficiency of the beam into radiative energy is determined by the expressions

$$K_{max} = (2\tilde{\alpha}\sigma\alpha_b^{1/2})^{1/2} \approx \frac{3}{2}\tilde{\alpha}^{1/2}\frac{R_b(x)}{R_b(0)}\left(\frac{J_b}{J_0}\right)^{1/4} \tag{46}$$

and for $a_b = 0.8$, $I_b = 0.1$ is about ~ 0.22; numerical calculations give 0.23.

We note that for the case where the field is switched on adiabatically, when for $\xi = 0$ we have $j_0 = 0$, the solution (43) takes a particularly simple form:

$$j^2 = \frac{j_{max}^2}{\mathrm{ch}[(2\tilde{\alpha}\alpha_b^{1/2}/\sigma)^{1/2}\xi]}, \qquad \rho^2 = \frac{\rho_{max}^2}{\mathrm{ch}[(2\tilde{\alpha}\alpha_b^{1/2}/\sigma)^{1/2}\xi]}. \tag{47}$$

The criterion for legitimacy of the expansion of the denominators in the system (33) reduces to the inequality $\tilde{\alpha}^{1/4}(\sigma\alpha_b^{1/2})^{3/4} \ll 1$, for the case of a low-current beam, which is fulfilled unconditionally.

In the range of high values of the electron beam current (column 1.8 of Table I), where we have $J_b \gg J_0$ ($\alpha_b\sigma^2 \gg 1$ and $\eta_0 = -\alpha_b\tau$), beam slowing can be ignored ($W = 0$), and Eqs. (41) have the form

$$\begin{gathered}\frac{d\rho}{d\xi} - i\cdot{}^3/_8\alpha_b^3\sigma^5|\rho|^2\rho = i\alpha_b\sigma^3 j,\\ \frac{dj}{d\xi} = -i\tilde{\alpha}\frac{\alpha_b}{\sigma}\rho.\end{gathered} \tag{48}$$

The structure of the solutions to Eqs. (48) is completely analogous to Eq. (43), with the sole difference that

$$\begin{gathered}j_{max} = 4\cdot\left(\frac{2}{3}\right)^{1/2}\frac{\tilde{\alpha}^{3/4}}{\alpha_b\sigma^4}, \qquad \rho_{max} = 4\cdot\left(\frac{2}{3}\right)^{1/2}\frac{\tilde{\alpha}^{1/4}}{\alpha_b\sigma^2},\\ y = \tilde{\alpha}^{1/2}\alpha_b\sigma\xi, \qquad \xi_0 = \frac{1}{\tilde{\alpha}^{1/2}\alpha_b\sigma}\ln\left(2^{3/2}\frac{j_{max}}{j_0}\right),\end{gathered} \tag{49}$$

while the conversion efficiency for beam energy into radiation is determined by the expressions

$$K_{max}=\frac{4}{3}\frac{\tilde{\alpha}^{1/2}}{\alpha_b\sigma^2}\approx\tilde{\alpha}^{1/2}\frac{R_b(0)}{R_b(x)}\frac{J_0}{J_b}. \tag{50}$$

In the case under discussion here, the criterion of applicability of Eq. (41), which contains only the cubic nonlinearity, reduces to the inequality $\tilde{\alpha}^{1/4}\ll 1$.

All the analytic results we have obtained are summarized in Table I. We note that for the case of the single-particle Cherenkov effect it is impossible to obtain an analytic solution; however, we can make approximate estimates,[3] which are also included in Table I.

Let us note once more that Table II contains characteristic results of numerical calculations for plasma amplifiers with real experimental parameters.[20]

Thus, the results of this paper imply that the use of beam-plasma waveguides with transverse density variation can lead to the creation of amplifier structures with gigawatt power capability.

[1)] By the "maximum amplification curve" we mean the geometric locus of points corresponding to the maximum amplification coefficient.

[1] A. F. Aleksandrov, M. V. Kuzelev, and A. N. Khalilov, Zh. Eksp. Teor. Fiz. **93**, 1714 (1987) [Sov. Phys. JETP **66**, 978 (1987)].

[2] A. F. Aleksandrov, M. V. Kuzelev, and A. N. Khalilov, Fiz. Plazmy **14**, 455 (1988) [Sov. J. Plasma Phys. **14**, 267 (1988)].

[3] M. V. Kuzelev and A. A. Rukhadze, *Electrodynamics of Dense Electron Beams in Plasmas* [in Russian], Nauka, Moscow, 1990.

[4] M. V. Kuzelev, F. Kh. Mukhametzyanov, and A. G. Shkvarunets, Fiz. Plazmy **9**, 1137 (1983) [Sov. J. Plasma Phys. **9**, 655 (1983)].

[5] M. V. Kuzelev, A. A. Rukhadze, P. S. Strelov *et al.*, Fiz. Plazmy **13**, 1370 (1987) [Sov. J. Plasma Phys. **13**, 793 (1987)].

[6] M. V. Kuzelev, F. Kh. Mukhametzyanov, M. S. Rabinovich *et al.*, Zh. Eksp. Teor. Fiz. **83**, 1358 (1982) [Sov. Phys. JETP **56**, 780 (1982)].

[7] M. B. Vinogradov, O. V. Rudenko, and A. P. Sukhorukov, *Theory of Waves* [in Russian], Nauka, Moscow, 1979.

[8] L. A. Vainshtein and V. A. Solntsev, *Lectures on Microwave Electronics* [in Russian], Sovetskoye Radio, Moscow, 1970.

[9] G. N. Watson, *A Treatise on the Theory of Bessel Functions*, 2nd Ed., Cambridge Univ. Press, 1966; Russian transl., Nauka, Moscow, 1949.

[10] L. D. Landau and I. M. Lifshits, *Fluid Mechanics*, Pergamon, Oxford, 1987; in Russian, Nauka, Moscow, 1986.

[11] M. V. Kuzelev, R. V. Romanov, I. A. Selivanov *et al.*, preprint from Inst. General Phys., USSR Acad. Sci. **23**, 1991.

[12] Yu. P. Bliokh, V. I. Karas', M. G. Lyubarskii *et al.*, Dokl. Akad. Nauk **275**, 56 (1984) [Sov. Phys. Dok. **29**, 205 (1984)].

[13] M. V. Kuzelev and A. A. Rukhadze, Usp. Fiz. Nauk **152**, 285 (1987) [Sov. Phys. Usp. **30**, 507 (1987)].

[14] V. D. Shapiro and V. I. Shevchenko, Izv. vuzov. Radiofizika **19**, 767 (1976).

[15] N. I. Aizatskii, Fiz. Plazmy **6**, 597 (1980) [Sov. J. Plasma Phys. **6**, 327 (1980)].

[16] M. V. Kuzelev, A. A. Rukhadze, and G. V. Sanadze, Zh. Eksp. Teor. Fiz. **85**, 1591 (1985) [Sov. Phys. JETP **62**, 921 (1985)].

[17] M. V. Kuzelev, A. A. Rukhadze, Yu. V. Bobylov, and V. A. Panin, Zh. Eksp. Teor. Fiz. **91**, 1620 (1986) [Sov. Phys. JETP **64**, 956 (1986)].

[18] M. V. Kuzelev, V. A. Panin, A. P. Plotnikov, and A. A. Rukhadze, Zh. Eksp. Teor. Fiz. **96**, 865 (1989) [Sov. Phys. JETP **69**, 491 (1989)].

[19] H. Wilhelmsson and J. C. Weiland, *Coherent Nonlinear Interactions of Waves in Plasmas*, Pergamon, Oxford, 1977; in Russian, Energoizdat, Moscow, 1981.

[20] I. A. Selivanov, A. V. Fedotov, and A. G. Shkvarunets, Proc. 8th Intl. Conf. on High-Power Particle Beams, Vol. 2, p. 1301. Novosibirsk, 1990.

Translated by Frank J. Crowne